Chinese Journal of Polymer Science Vol. 32, No. 6, (2014), 805–816

Chinese Journal of Polymer Science

In Vivo Degradation Behavior of Porous Composite Scaffolds of Poly(lactide-*co*-glycolide) and Nano-hydroxyapatite Surface Grafted with Poly(L-lactide)*

Yu-feng Tang and Jian-guo Liu**
First Hospital, Jilin University, Changchun 130021, China
Zong-liang Wang, Yu Wang, Li-guo Cui, Pei-biao Zhang** and Xue-si Chen
Key Laboratory of Polymer Ecobiomaterials, Changchun Institute of Applied Chemistry, Graduate School of Chinese Academy of Sciences, Chinese Academy of Sciences, Changchun 130022, China

Abstract The biodegradable porous composite scaffold, composed of poly(lactide-*co*-glycolide) (PLGA) and hydroxyapatite nanoparticles (n-HAP) surface-grafted with poly(L-lactide) (PLLA) (g-HAP) (g-HAP/PLGA), was fabricated using the solvent casting/particulate leaching method, and its *in vivo* degradation behavior was investigated by the intramuscular implantation in rabbits. The composite of un-grafted n-HAP/PLGA and neat PLGA were used as controls. The scaffolds had interconnected pore structures with average pore sizes between 137 μm and 148 μm and porosities between 83% and 86%. There was no significant difference in the pore size and porosity among the three scaffolds. Compared with n-HAP/PLGA, the thermo-degradation temperature (T_c) of g-HAP/PLGA decreased while its glass transition temperature (T_g) increased. The weight change, grey value analysis of radiographs and SEM observation showed that the composite scaffolds of g-HAP/PLGA and n-HAP/PLGA showed slower degradation and higher mineralization than the pure PLGA scaffold after the intramuscular implantation. The rapid degradation of PLGA, g-HAP/PLGA and n-HAP/PLGA occurred at 8–12 weeks, 12–16 weeks and 16–20 weeks, respectively. Compared with n-HAP/PLGA, g-HAP/PLGA showed an improved absorption and biomineralization property mostly because of its improved distribution of HAP nanoparticles. The levels of both calcium and phosphorous in serum and urine could be affected to some extent at 3–4 weeks after the implantation of g-HAP/PLGA, but the biochemical detection of serum AST, ALT, ALP, and GGT as well as BUN and CRE showed no obvious influence on the functions of liver and kidney.

Keywords: Nanocomposite; Surface modification; Absorption; Biomineralization; Biochemical detection.

INTRODUCTION

Hydroxyapatite (HA) ceramics have been employed widely as bone substitutes for the clinical orthopaedic application because of their biocompatibility, mechanical stability and direct bone-bonding ability[1–4]. However, HA ceramics still have disadvantages as bone substitutes, such as brittleness, poor processability and minimal degradability[2]. The composites of nano-sized HA (n-HA) and biodegradable polyesters, such as poly(lactic acid) (PLA)[4], poly(glycolic acid) (PGA) and their copolymer poly(lactide-*co*-glycolide) (PLGA)[5], have attracted much attention recently for the advantages of improved mechanical properties, processability and

* This work was financially supported by the National Natural Science Foundation of China (Nos. 51273081, 51103149 and 51273195), the Project of International Cooperation from the Ministry of Science and Technology of China (No. S2013GR04340), and the Major Project of Science and Technology of Jilin Province (20130201005GX).
** Corresponding authors: Jian-guo Liu (刘建国), E-mail: jgliu.2005@yahoo.com.cn
Pei-biao Zhang (章培标), E-mail: zhangpb@ciac.ac.cn
Received December 27, 2013; Revised February 11, 2014; Accepted February 17, 2014
doi: 10.1007/s10118-014-1454-5

absorbability[6]. Among these composites, n-HA/PLGA is one of the most promising bone materials because the mechanical properties and biodegradation rate of PLGA matrix can be manipulated in some extent by controlling the molecular weight of the copolymer and the ratio of lactide to glycolide in the copolymer[7–9].

The degradation behavior of bone materials is one of the key factors in bone tissue engineering because it is directly associated with the bone tissue ingrowth and bone regeneration after the implantation for the repair of bone defects[10–12]. The biomaterial should not only stimulate and support tissue growth, but it may also degrade with the same rate as the generation of new tissues. If the degradation rate of the implant matches the rate of tissue growth, it will provide enough spaces for cell migration, proliferation and matrix formation[13]. Guarino *et al.* showed that the incorporation of n-HA into polymers could alter some physical properties, such as the crystallinity, hydrophilicity and mechanical properties of polymers so as to influence the *in vitro* or *in vivo* degradation[14].

Meanwhile, the matrix/particle interface in composites can also change the materials' degradation behavior. Delabarde *et al*. reported that addition of well-dispersed n-HA particles in bulk material resulted in increased rate of mass loss during aging, which was identified as the accelerated degradation at the matrix/particle interface[15]. We also reported that the surface modification of n-HA by grafting poly(L-lactide) (PLLA) could further improve the interface binding between the nanoparticles and the polymer matrix, and the dispersion of the nanoparticles in chloroform or polymer matrix[8, 16]. The composite materials of the modified n-HA and PLLA or PLGA were verified to exhibit an improved thermal stability and mechanical properties. However, few researchers have evaluated the *in vivo* degradation property of porous materials, especially the porous nanocomposite of n-HA/PLGA.

The *in vivo* degradation is a complicated procedure for porous HA composite scaffolds. It is related to the integrative outcome of material's absorption, mineral deposition and tissue ingrowth[17]. In this study, the biodegradable porous composite scaffolds, composed of PLGA and grafted or ungrafted n-HAP, were fabricated and implanted intramuscularly, and the *in vivo* degradation behaviors of the implants were evaluated and compared by mass change assessment combined with the analysis of grey value of X-ray, SEM observation and biochemical detection. Meanwhile, the novel evaluation methods and the relationship between mineralization and biodegradation were explored.

MATERIALS AND METHODS

Preparation and Characterization of Porous Scaffolds

Poly(lactide-*co*-glycolide) (PLGA, LA/GA = 80:20, M_w = 196000), hydroxyapatite nano-particles (n-HAP) and PLLA surface-grafted hydroxyapatite nano-particles (g-HAP) were synthesized and employed in this study[8, 18]. The porous scaffolds of g-HAP/PLGA, n-HAP/PLGA and PLGA were fabricated using the solvent casting/particulate leaching method according to our previous work[16]. The content of g-HAP or n-HAP was 10 wt% in the composite. The sucrose particles were 100–450 μm in diameter and the mass ratio of composites, or PLGA/sucrose, was 1:6 (*W*/*W*). Pure PLGA was used as control. The obtained porous disks were cut into small bars of 3 mm × 20 mm, and sterilized with UV irradiation for the following study. The pore size and porosity of scaffolds were measured by SEM observation[17] and liquid displacement method[19]. The thermal stability of the samples was determined using thermogravimetry analysis (TGA) (TA Instruments TGA500, USA). About 10 mg of each sample was heated under nitrogen atmosphere at the heating rate of 20 K/min and the measurements were recorded from 30 °C to 800 °C. Meanwhile, the thermal properties of the samples were measured with the differential scanning calorimetry (DSC) (TA Instruments DSC100, USA) at a heating rate of 10 K/min from 30 °C to 200 °C under the protection of nitrogen atmosphere.

Intramuscular Implantation

The pre-weighed cell-free porous implants were embedded into the dorsal muscles of 18 rabbits by surgery. Three parallel samples in a rabbit were used for each material. Animals were kept in the Institute of Experimental Animal of Jilin University, in accordance with the institutional guidelines for care and use of

laboratory animals. After surgery, the rabbits were sacrificed with air injection at 4, 8, 12, 16 and 20 weeks. The implants were taken out and then fixed with 4% paraformaldehyde for 2 h at room temperature. The samples were washed with distilled water three times and freeze-dried for 48 h. The weight loss ratio and the relative weight ratio of the implants were calculated with the following equations:

Weight loss ratio (%) = (weight before surgery – weight after surgery)/ weight before surgery × 100%

Relative weight ratio (%) = weight after surgery / weight before surgery × 100%

Computer Radiographs

The *in vivo* intramuscular implants of g-HAP/PLGA, n-HAP/PLGA and PLGA scaffolds for 4, 8, 12, 16 and 20 weeks postsurgery were examined with CR. The CR digital images were analyzed with NIH Image J software. Mean grey value and max grey value were obtained for assay the mineralization of the implants.

Emission Scanning Electron Microscope (ESEM) Analysis

The porous scaffolds and the freeze-dried samples were cut and coated with Au/Pd in a sputter coater. The microstructures of the scaffolds and the intramuscular implants were studied under an emission scanning electron microscope (ESEM) (Philips XL30 ESEM FEG, Japan). The pore diameters of total 200 pores for each material before implantation and the pore area fractions of 5 SEM images for each material after implantation were measured with NIH Image J.

Biochemical Detection of Serum and Urine

The concentrations of calcium (Ca^{2+}) and inorganic phosphorus (P^{3+}) in serum and urine of rabbits implanted with tissue engineered g-HA/PLGA were monitored using an autoanalyzer (Hitachi 747, Hitachi, Japan) after surgery. The serum samples were obtained at 0 week (before surgery), 1 week, 4 weeks and 10 weeks postsurgery, and the urine samples were collected at 0 week (before surgery), 1 week, 3 weeks and 5 weeks postsurgery. The samples obtained from the rabbits before surgery were used as the control. Meanwhile, serum aspartate aminotransferase (AST), alanine aminotransferase (ALT), alkaline phosphatase (ALP) and gamma-glutamyltransferase (GGT), as well as blood urea nitrogen (BUN) and creatinine (CRE) were detected using the autoanalyzer before and after surgery.

Statistical Analysis

All quantitative data were analyzed with Origin 8.0 (OriginLab Corporation, USA) and expressed as the mean ± standard deviation. Statistical comparisons were carried out by analysis of One-way Variance (ANOVA, Origin7.0). A value of $p < 0.05$ was considered to be statistically significant.

RESULTS AND DISCUSSION

Scaffold Preparation and Characterization

Figures 1(a–c) show the SEM micrographs of g-HAP/PLGA, n-HAP/PLGA and PLGA porous scaffolds fabricated using the solvent casting/porogen leaching method. There are several methods that have been developed to fabricate 3D polymeric scaffolds for tissue engineering application, such as phase separation, gas foaming, electrical spinning, fiber bonding and porogen leaching[20–23]. Among them, the solvent casting/porogen leaching is a traditional and popular method for fabricating porous scaffolds[23]. The pore size and porosity of scaffolds can be controlled easily using this method through adjusting the size of soluble particulates and the ratio of particulate to polymer. Usually, water soluble particulates such as salts and carbohydrates are used as the porogen materials[24]. Sucrose is more suitable for the solvent casting than salt because its lower density prevents particles from sinking quickly to the solution bottom. Thus, more uniform pore structures and higher porosity (more than 85%) can be reached by use of sucrose as particulate[25]. Our results showed that the pores of all samples were interconnected and irregular. The porosities were 83.6% – 86.6% and the average pore diameters were 137.3–148.2 μm[17]. According to the pore size distribution shown in Figs. 1(d–f), g-HAP/PLGA and n-HAP/PLGA composite scaffolds had a larger portion of pores with the diameter > 300 μm than pure PLGA scaffolds.

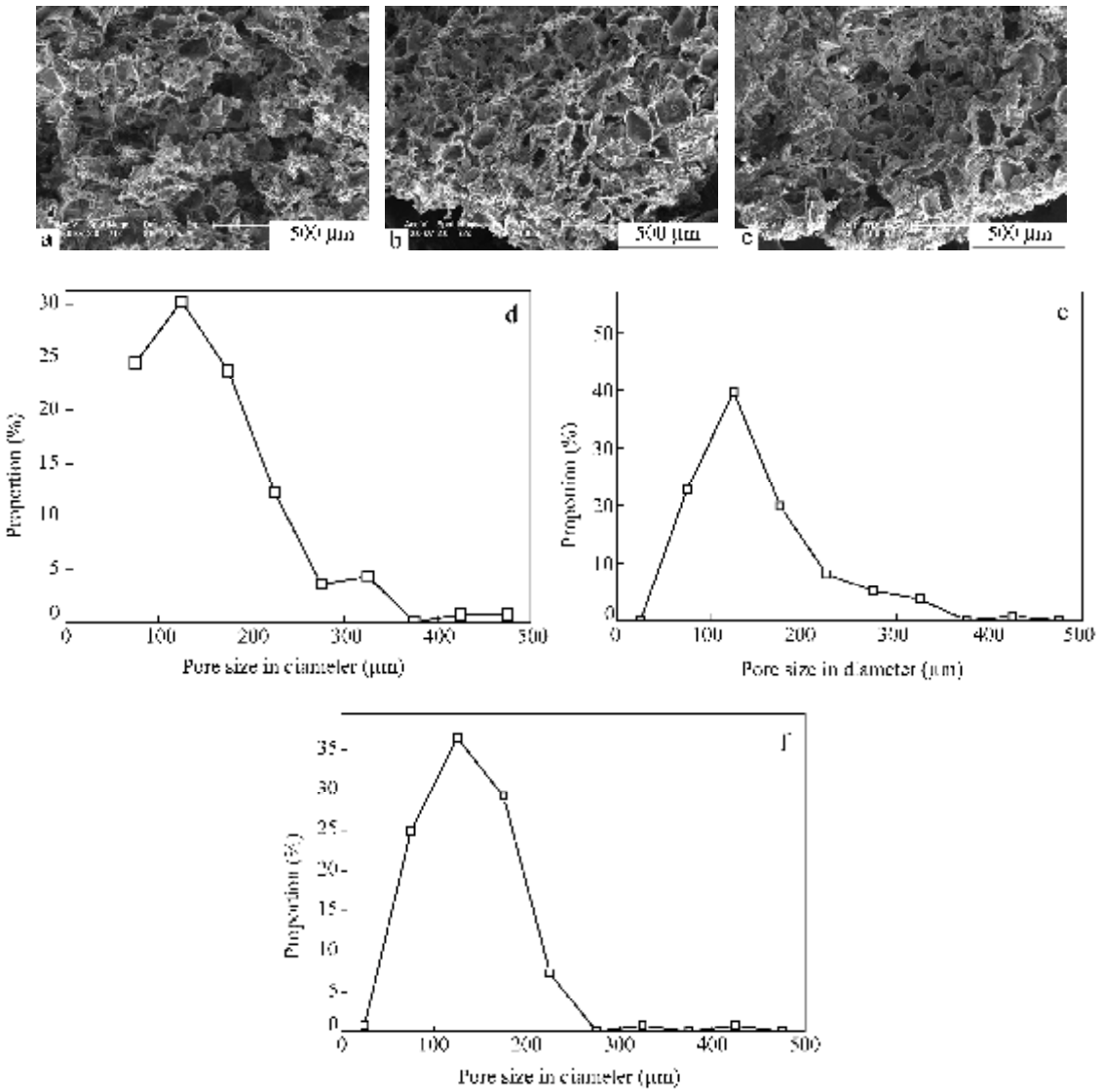

Fig. 1 SEM micro-photographs (a–c) and the pore size distribution (d–f) of porous scaffolds of g-HAP/PLGA (a and d), n-HAP/PLGA (b and e) and PLGA (c and f) fabricated with the solvent casting/particulate leaching method

Thermostability Analyzed with TGA and DSC

As shown in Fig. 2, the thermal properties of g-HAP/PLGA, n-HAP/PLGA and PLGA were analyzed with TGA and DSC. The TGA curves in Fig. 2(a) showed that both g-HAP/PLGA and n-HAP/PLGA composites had two decomposition steps, which were different from the pure PLGA with only one decomposition step. For n-HAP/PLGA composite, the first decomposition step was at 223.8 °C and had 44.8% weight loss, and the second decomposition step was at 369.3 °C and had 38.8% weight loss. But for g-HAP/PLGA composite, the first decomposition step was at 221.5 °C and had 45.9% weight loss, and the second decomposition step was at 350.6 °C and had 36.8% weight loss. The decomposition temperature of PLGA was 288.0 °C. The results indicated that the thermal stability of scaffolds was affected by the incorporation of n-HAP, and the surface modification of n-HAP with PLLA slightly decreased the thermal stability.

The DSC curves in Fig. 2(b) showed that the glass transition temperature (T_g) of g-HAP/PLGA, n-HAP/PLGA and PLGA was 66.1 °C, 62.0 °C and 52.0 °C, respectively. The T_g of g-HAP/PLGA increased compared to that of n-HAP/PLGA and PLGA. It was deduced that the different thermal properties between

g-HAP/PLGA and n-HAP/PLGA might result from the improved distribution of grafted g-HAP nanoparticles in polymer matrix.

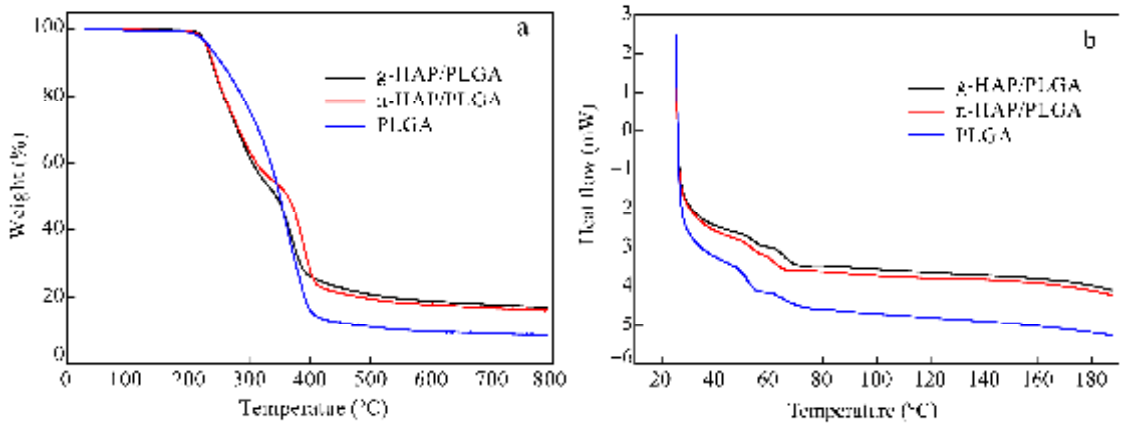

Fig. 2 TGA and DSC curves of the porous scaffolds of g-HAP/PLGA, n-HAP/PLGA and PLGA

In Vivo Biodegradation

The *in vivo* biodegradation of g-HAP/PLGA, n-HAP/PLGA, and PLGA scaffolds was investigated by intramuscular implantation in rabbits, and analyzed integratively with optical observation, weight loss and relative weight at different time intervals. The numbers of destroyed implants, that an implanted scaffold was destroyed into more than 3 pieces because of degradation, are shown in Table 1. Typically, the implants of PLGA exhibited a faster degradation than those of g-HAP/PLGA and n-HAP/PLGA. The destroyed scaffolds of PLGA appeared partly (1/3) at 8 weeks and wholly (3/3) at 12 weeks. Both g-HAP/PLGA and n-HAP/PLGA composite scaffolds began to present the first destroyed scaffold at 16 weeks, but g-HAP/PLGA presented more destroyed scaffolds (2/3) than n-HAP/PLGA (1/3) at this time interval. At 20 weeks, there were only 2/3 but not all implants were destroyed in these two groups because one of the three implants for each material was mineralized completely. The results indicated that g-HAP/PLGA degraded faster than n-HAP/PLGA although both of them had the similar ability of biomineralization.

Table 1. The degradation observation of g-HAP/PLGA, n-HAP/PLGA and PLGA porous scaffolds implanted intramuscularly at different time intervals

Implants	Number of destroyed implants*					
	n	4 weeks	8 weeks	12 weeks	16 weeks	20 weeks
g-HAP/PLGA	3	0	0	0	2/3	2/3
n-HAP/PLGA	3	0	0	0	1/3	2/3
PLGA	3	0	1/3	3/3	3/3	3/3

* The destroyed implants mean that the implanted scaffold was destroyed into more than 3 pieces because of degradation

As shown in Fig. 3, the weight changes of the implants, including the weight loss (Fig. 3b) and the relative weight (Fig. 3c), were employed to quantitatively assess *in vivo* degradation of different materials. Quantification of weight loss is one of the most popular approaches employed for assessing the degradability of biomaterials[26, 27]. Figure 3(b) shows the weight loss of the implants at 4–20 weeks postsurgery. At 4 weeks, the weight loss of g-HAP/PLGA was 57.9 ± 12.3% and higher than those of n-HAP/PLGA (38.4 ± 13.7%) and PLGA (19.1 ± 16.9%), and the difference between g-HAP/PLGA and PLGA was significant ($p < 0.05$). At the following time intervals, the weight loss of g-HAP/PLGA was similar to those of PLGA but higher than that of n-HAP/PLGA. However, at all time intervals, there were no significant differences in the weight loss between g-HAP/PLGA and n-HAP/PLGA ($p > 0.05$).

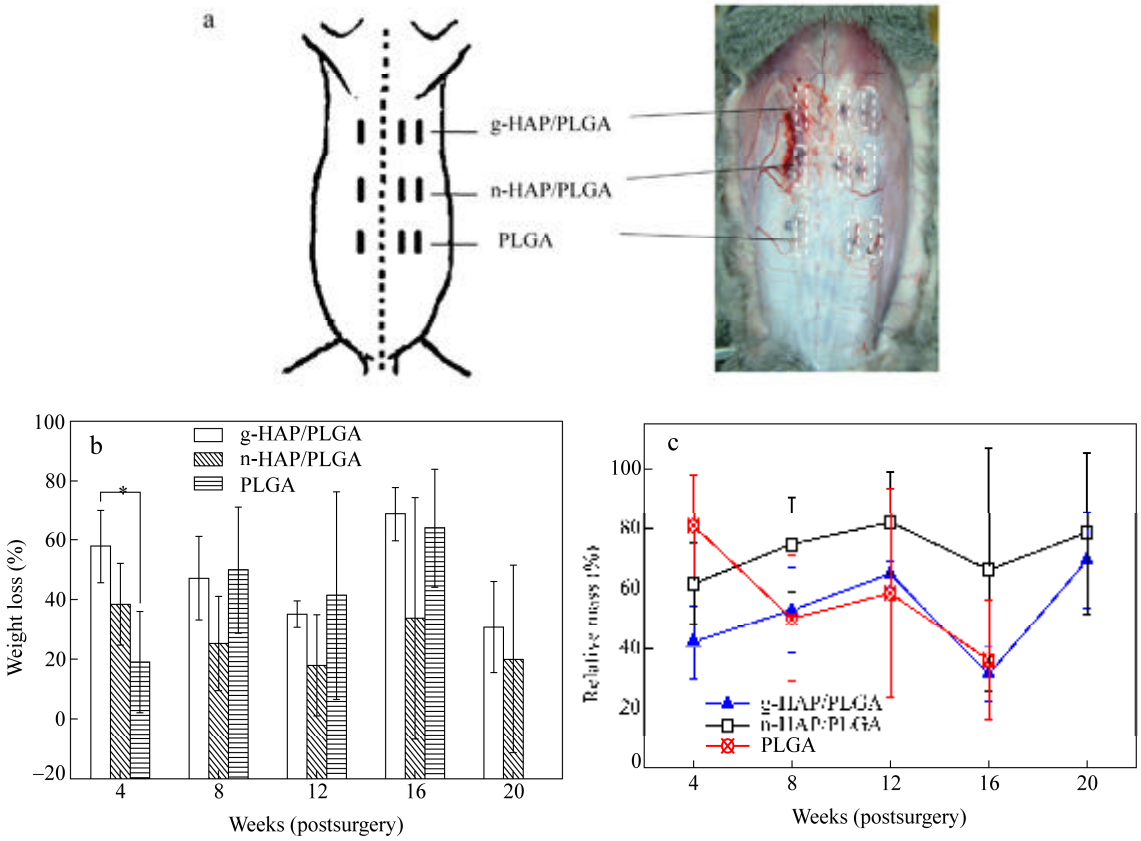

Fig. 3 Animal test: (a) the implant distributions of g-HAP/PLGA, HAP/PLGA and PLGA porous scaffolds embedded into rabbit dorsal muscles (Each material had three parallel samples in a rabbit.); (b) weight loss ratio and (c) relative weight ratio of the intramuscular implants of g-HAP/PLGA, n-HAP/PLGA and PLGA scaffolds for 4–20 weeks postsurgery. (* $p < 0.05$ compared to the other group, $n = 3$.)

To describe better the weight changes of the porous implants *in vivo*, the relative weights, the weight of an implant pre-surgery compared to that postsurgery, were suggested in present study and shown in Fig. 3(c). Except for material degradation, the final weight of a porous implant was determined by calcium deposition, and cells migrating into the scaffold and extracellular matrix (ECM) formation because of its complex *in vivo* processes[17]. Thus, the relative weight of an implant is also regarded as a valuable and comprehensive assessment for its *in vivo* process, especially the assessment for the balance among degradation, mineralization and osteogenesis of bone materials. At 4 weeks postsurgery, the relative weight of g-HAP/PLGA decreased steeply and was lower than that of PLGA ($p < 0.05$) and HA/PLGA ($p > 0.05$). The larger mass loss of the composite implants of g-HAP/PLGA at the initial stage might be associated to the rapid material degradation and release of retained sucrose from scaffolds because of its higher opening porosity and larger pore size. At the following stages, the relative weights of g-HAP/PLGA and n-HAP/PLGA composites increased gradually and rose up to a peak (64.9 ± 4.4% and 82.0 ± 16.9%, respectively) at 12 weeks, which was nearly by 65.0% increased than that at 4 weeks. However, the relative weights of all three materials decreased greatly at 16 weeks postsurgery. PLGA scaffolds were then absorbed completely and those of the composite scaffolds resumed up at 20 weeks (the levels were similar to those at 12 weeks). The results indicated that the largest degradation rate for PLGA matrix occurred at this stage (during 12 weeks – 16 weeks) and the scaffolds were replaced with the ingrown tissues at 20 weeks. The relative weights of g-HAP/PLGA were 20% lower than those of n-HAP/PLGA at the time intervals before 12 weeks and changed nearly at the same levels as the PLGA at the time intervals of 4 weeks – 16 weeks. But g-HAP/PLGA had more decreased relative weights (17.8% higher than that of

n-HAP/PLGA) at 16 weeks and more increased relative weights (25.9% higher than that of n-HAP/PLGA) at 20 weeks compared to n-HAP/PLGA. The gap in relative weight between g-HAP/PLGA and n-HAP/PLGA was shortened to 9.1% at 20 weeks. It is deduced that g-HAP/PLGA had an improved absorption ability compared to n-HAP/PLGA because of the uniform distribution of HA nanoparticles in the polymer matrix after surface modification.

The Relationship between Mineralization and Biodegradation

The mean grey values of the computer radiographs of the intramuscular implants were analyzed using NIH image J for assay of the relationship between *in vivo* biodegradation and biomineralization of the composite scaffolds. X-ray radiograph is a routine clinical examination in orthopaedics. In general, more mineralization formed in the bone implant, higher grey value will be shown in the radiograph image. In our previous work, the mineralization has been observed at local areas by X-ray radiographs at the initial stages[17].

As shown in Fig. 4(a), the mean grey values of PLGA were higher at 4 weeks and 8 weeks postsurgery but lower at 12 weeks than those of g-HAP/PLGA and n-HAP/PLGA, and the differences at 4 weeks and 12 weeks were statistically significant ($p < 0.05$). At the initial stages of 4 weeks and 8 weeks, the higher grey value of the implants for PLGA may result from the higher density of scaffold. The mean grey values of the three materials kept at the similar levels from 4 weeks to 8 weeks but decreased greatly (nearly 50%) at 12 weeks. There was no significant difference in mean grey values between g-HAP/PLGA and n-HAP/PLGA ($p > 0.05$) before 12 weeks postsurgery. Combined with the results of weight loss analysis, it is deduced that the materials (mainly PLGA matrix) began to degrade at 12 weeks and the degradation rate reached the maximal at 16 weeks. At 16 weeks postsurgery, the mean grey values of all materials increased largely. Among them, the composite of g-HAP/PLGA exhibited the highest values, which was 159.3% higher than that at 4 weeks and 637.5% higher than that at 12 weeks. The difference of mean grey values at 16 weeks between PLGA and g-HAP/PLGA or n-HAP/PLGA was statistically significant ($p < 0.05$). At 20 weeks postsurgery, the mean grey values of g-HAP/PLGA increased constantly but those of n-HAP/PLGA and PLGA decreased slightly. The results indicated that the strongest biomineralization of the nanocomposite scaffolds might occur at the period of the rapidest degradation rate.

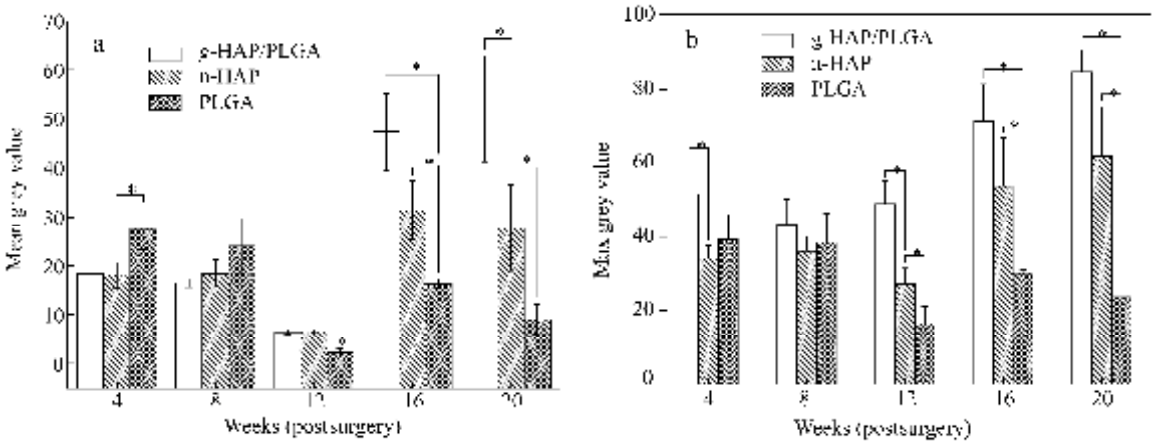

Fig. 4 Mean grey values (a) and max gray values (b) of computer radiographs (CR) of the intramuscular implants at different time intervals analyzed with NIH Image J software ($^{*}p < 0.05$ compared to the other group, $n = 3$.)

Meanwhile, the max grey values of all implants were further analyzed to investigate the difference in local mineralization between g-HAP/PLGA and n-HAP/PLGA. Figure 4(b) shows that the max grey values of g-HAP/PLGA were higher than those of n-HAP/PLGA and PLGA at all time intervals, and the differences were significant at 4 weeks and 12 weeks compared to n-HAP/PLGA ($p < 0.05$), and at 12–20 weeks compared to PLGA ($p < 0.05$). In the groups of g-HAP/PLGA and n-HAP/PLGA, there was a great increase of the max grey

values at 16–20 weeks postsurgery for their biomineralization. However, the max grey values of PLGA decreased obviously at 12–20 weeks postsurgery due to its degradation and lack of biomineralization ability. It indicated that the surface modification of n-HAP with PLLA could improve the local mineralization of g-HAP/PLGA because of its improved distribution of HA nanoparticles. The local mineralization of g-HAP/PLGA might start from 4 weeks postsurgery or earlier but the general mineralization only occurred after 12 weeks postsurgery when the polymer matrix degraded rapidly and largely.

Microstructure Changes Observed by SEM

After implantation, the degradation of the biodegradable polymer scaffolds can result in the microstructure change. The pore structures will be destroyed gradually and replaced with the ingrowth tissues. Thus, themicrostructure stability is a key factor for biodegradable porous scaffolds providing space or mechanical supports for tissue ingrowth in the regeneration process[28, 29]. Meanwhile, the tissue ingrowth of a scaffold is also associated with its biocompatibility, pore size and pore interconnection[30, 31]. Figure 5 shows SEM photographs of the intramuscular implants at the different time intervals (8 weeks, 12 weeks and 20 weeks postsurgery). At 8 weeks postsurgery, most macropores (> 100 μm) kept their original shapes and a few of pores filled with newly ingrown tissues were observed in the groups of g-HAP/PLGA and n-HAP/PLGA. The former seemed to be better in keeping pore structure than the latter. At 12 weeks postsurgery, the pore sizes of g-HAP/PLGA and n-HAP/PLGA were getting smaller and the quantities of pores decreased a lot due to the degradation and tissue ingrowth. At 20 weeks postsurgery, the pore structures of g-HAP/PLGA disappeared while the pore sizes of n-HAP/PLGA continued to get smaller. The scaffold of g-HAP/PLGA was replaced with layers of newly formed tissues. Compared with the composite scaffolds, the pore structures of PLGA scaffold were destroyed mostly at 8 weeks and disappeared completely at 12 weeks due to its quick degradation rate.

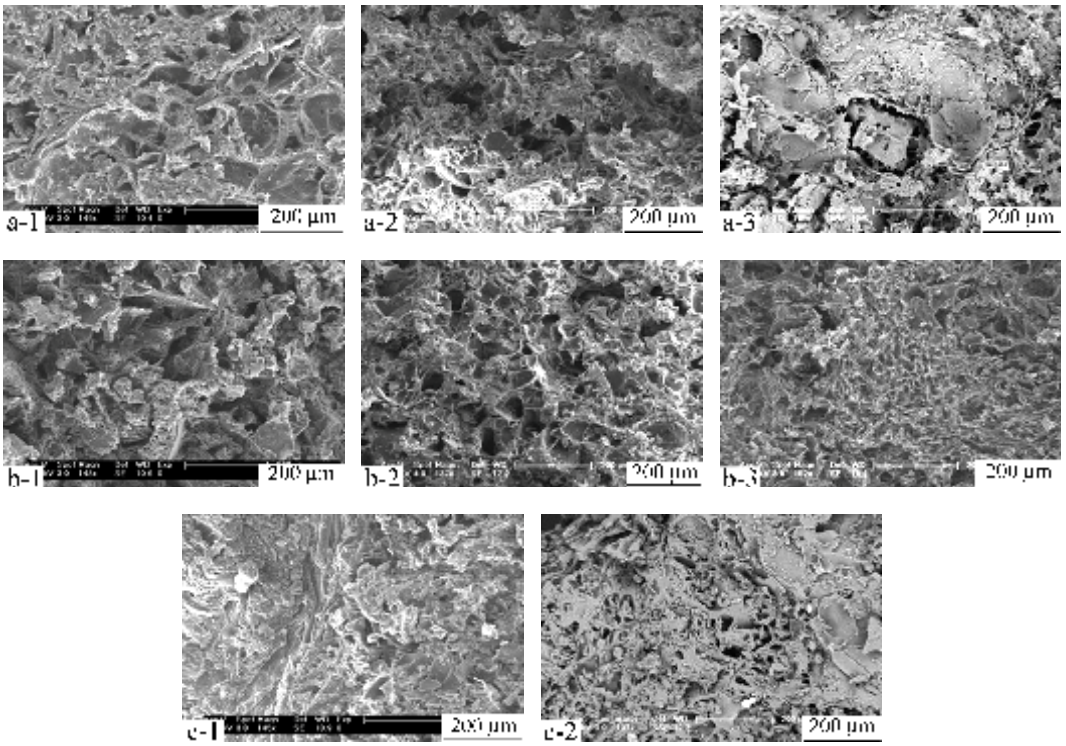

Fig. 5 SEM micrographs of the intramuscular implants of g-HAP/PLGA (a-1–a-3), n-HAP/PLGA (b-1–b-3) and PLGA (c-1, c-2) at 8 weeks (-1), 12 weeks (-2) and 20 weeks (-3) postsurgery

As shown in Fig. 6, the 2D pore area fraction was further employed in present study by analysis of SEM micrographs with NIH Image J software to quantitatively assess the microstructure changes of the implants. The results showed that the pore area fractions of g-HAP/PLGA, n-HAP/PLGA and PLGA at 8 weeks were 63.6 ± 3.9%, 63.3 ± 6.3% and 62.1 ± 6.9%, respectively, and there was little difference among the three implants. However, at 12 weeks, the pore area fraction of g-HAP/PLGA decreased to 56.6 ± 6.2% mainly corresponding to tissue ingrowth and was slightly lower than that of n-HAP/PLGA (72.5 ± 6.3%) ($p > 0.05$). Compared to that of n-HAP/PLGA, the pore area fraction of PLGA decreased a lot ($p < 0.05$) because its pore structure mostly collapsed. At 20 weeks, the pore area fractions of both g-HAP/PLGA and n-HAP/PLGA decreased and the pore area fraction of g-HAP/PLGA was significantly lower than that of n-HAP/PLGA ($p < 0.05$). According to SEM observation, the pore structure of g-HAP/PLGA collapsed completely at this time. The result of area fraction analysis was consistent with the observation of SEM micrographs. It indicated that the pore area fraction analysis based on SEM micrographs could be used as quantitative assessment for *in vivo* stability and degradation of porous scaffolds.

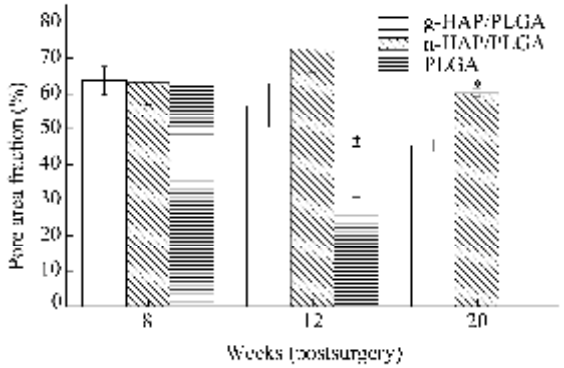

Fig. 6 Pore area fraction of the SEM micrographs of the intramuscular implants at 8 weeks, 12 weeks and 20 weeks postsurgery (* $p < 0.05$ compared to the other groups, $n = 5$.)

Calcium and Inorganic Phosphor in Serum and Urine

The concentrations of Ca^{2+} and P^{3+} in serum (Fig. 7a) and urine (Fig. 7b) of rabbits implanted with g-HAP/PLGA before or after surgery were monitored. Figure 7(a) shows that the serum concentrations of Ca^{2+} and P^{3+} before surgery were 3.57 ± 0.20 mmol/L and 1.55 ± 0.42 mmol/L respectively, and the ratio of Ca^{2+}/P^{3+} was 2.45 ± 0.74. There were slight changes in the serum levels of Ca^{2+} and P^{3+} at 1 week, 4 weeks and 10 weeks postsurgery compared to those before surgery ($p > 0.05$). The concentration of Ca^{2+} decreased at 4 weeks and 10 weeks while the concentration of P^{3+} increased at 10 weeks. Thus, the ratios of Ca/P in serum decreased gradually after surgery and reached to 1.66 ± 0.05 at 10 weeks. However, as shown in Fig. 7(b), the urine concentrations of Ca^{2+} and P^{3+} increased significantly at 3 weeks (1.82 ± 0.27 mmol/L and 1.18 ± 0.16 mmol/L) compared to those before surgery (0.82 ± 0.19 mmol/L and 0.72 ± 0.06 mmol/L, respectively) ($p < 0.05$), which were greatly different from those in serum. At 5 weeks, the Ca^{2+} level continuously increased to 2.04 ± 0.31 mmol/L but the P^{3+} level returned slightly (0.91 ± 0.34 mmol/L). The results indicated that the implantation of HA composite materials affected the levels of both Ca^{2+} and P^{3+} in serum and urine to some extent at 3–4 weeks after surgery. It may result from the surgical injury, the absorption of HA materials and the need of bone reconstruction.

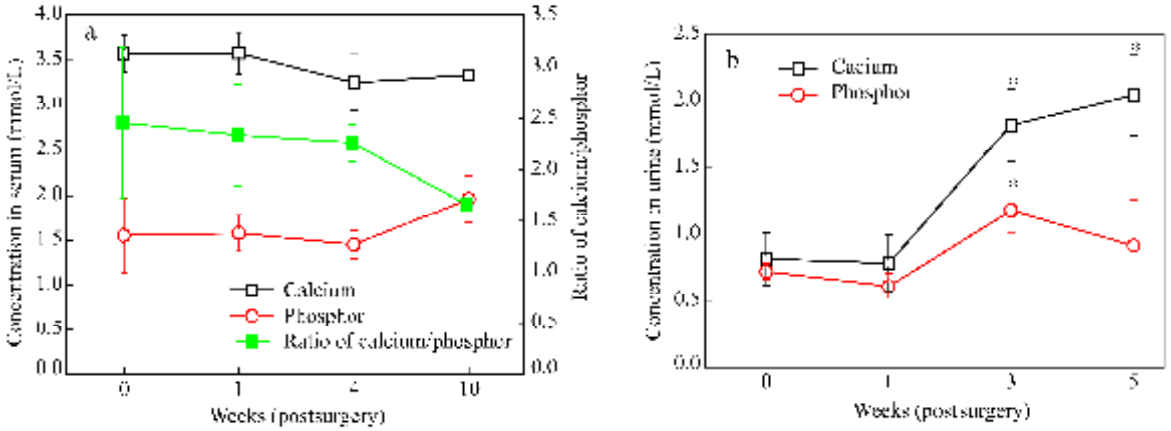

Fig. 7 Concentrations of calcium and phosphor in serum (a) and urine (b) of rabbits intramuscularly implanted with g-HAP/PLGA nanocomposites (* $p < 0.05$ compared to the other group, $n = 5$.)

Biochemical Changes of Liver and Kidney

As shown in Fig. 8, the serum biochemical detection was undertaken to monitor the negative effects of implanted g-HAP/PLGA on the function of rabbit liver and kidney. Before surgery, the activity of AST, ALT, ALP, and GGT was 23.0 ± 10.1 U/L, 24.7 ± 8.1 U/L, 27.5 ± 14.2 U/L and 3.8 ± 3.1 U/L, respectively. The activity of AST and ALT increased slightly at 1 week postsurgery ($p > 0.05$), and then decreased significantly at 4 weeks and 10 weeks postsurgery ($p < 0.05$). The activity of ALP increased from 1 week to 10 weeks after surgery compared to that before surgery but there were no significant differences among them ($p > 0.05$). The activity of GGT decreased a little after 1 – 4 weeks and then increased at 10 weeks postsurgery. ALP is an enzyme found in the liver, kidney, bone and teeth. The serum ALP mainly came from the bone but the serum GGT, ALT and AST were mainly from the liver. The results of present study indicated that the slight increase of ALP and the decrease of GGT, ALT and AST might result from the damage of bone after surgery, and the implantation of g-HAP composite didn't affect the function of liver.

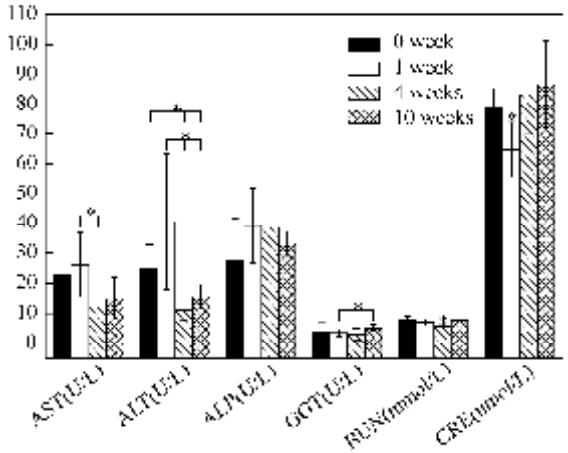

Fig. 8 Concentration of AST, ALT, ALP, ALP, GGT, BUN and GRE in serum of rabbits intramuscularly implanted with nanocomposites (* $p < 0.05$ compared to the other group, $n = 5$.)

BUN and CRE represent the function of kidney. High levels of BUN and CRE might be caused by kidney damage. The concentration of BUN decreased slightly after surgery, and there was a significant decrease at 3 weeks ($p < 0.05$). Meanwhile, the concentration of CRE decreased significantly at 1 week after surgery ($p < 0.05$), and slightly increased at 4 weeks and 10 weeks ($p > 0.05$). It is well known that CRE is a non-protein

waste product of creatine phosphate metabolism by skeletal muscle tissue and the serum concentration of CRE is proportional to muscle mass[32]. The results indicated that the function of kidney was not affected by the implantation of the porous nanocomposite, and the decrease of BUN and CRE might be caused by the muscle damage during surgery.

CONCLUSIONS

The *in vivo* degradation behavior of porous composite scaffolds of surface grafted g-HAP/PLGA compared with those of ungrafted n-HAP/PLGA and pure PLGA was investigated by intramuscular implantation. The surface modification of n-HAP with PLLA didn't affect the microstructure of the composite scaffold but would change the thermal properties slightly, including decreasing the decomposition temperature and increasing the glass transition temperature. After intramuscular implantation, the composite scaffolds of g-HAP/PLGA and n-HAP/PLGA presented slower degradation and higher mineralization rates compared to the pure PLGA scaffolds. The rapid degradation of PLGA, g-HAP/PLGA and n-HAP/PLGA occurred at 8–12 weeks, 12–16 weeks and 16–20 weeks, respectively. Compared with n-HAP/PLGA, g-HAP/PLGA showed an improved absorption and biomineralization because of its improved distribution of g-HAP nanoparticles in PLGA matrix. The levels of both Ca^{2+} and P^{3+} in serum and urine could be affected to some extent at 3–4 weeks after the implantation of g-HAP/PLGA due to the surgical injury, the absorption of HA materials and the need of bone reconstruction, but the biochemical detection showed that no obvious influences on the function of liver and kidney were observed. From the results, it was concluded that the porous composite of g-HAP/PLGA, PLGA incorporated with HA nanoparticles after surface grafting with PLLA, could be used as a prospective scaffold or bone substitute for bone tissue engineering and bone repair because of its improved *in vivo* absorption and biomineralization.

REFERENCES

1 Tamai, N., Myoui, A., Kudawara, I., Ueda, T. and Yoshikawa, H., J. Orthop. Sci., 2010, 15: 560
2 Furukawa, T., Matsusue, Y., Yasunaga, T., Shikinami, Y., Okuno, M. and Nakamura, T., Biomaterials, 2000, 21: 889
3 Mate-Sanchez, de.Val. J.E., Mazon, P., Guirado, J.L., Ruiz, RA., Ramirez Fernandez, M.P. and Negri, B., J. Biomed. Mater. Res A., 2012, 100A: 3446
4 Zhang, C.Y., Lu, H., Zhuang, Z., Wang, X.P. and Fang, Q.F., J. Mater. Sci. Mater. Med., 2010, 21: 3077
5 Lv, Q., Nair, L. and Laurencin, C.T., J. Biomed. Mater. Res A., 2009, 91: 679
6 Cui, Y., Liu, Y., Jing, X., Zhang, P. and Chen, X., Acta Biomater., 2009, 5: 2680
7 Kim, S.S. Sun, Park, M., Jeon, O., Yong, C.C. and Kim, B.S., Biomaterials, 2006, 27: 1399
8 Hong, Z., Zhang, P., Liu, A., Chen, L., Chen, X. and Jing, X., J. Biomed. Mater. Res A., 2007, 81: 515
9 Vasita, R., Shanmugam, K. and Katti, D.S., Polym. Degrad. Stab., 2010, 95: 1605
10 Xie, X.H., Wang, X.L, Zhang. G., He, Y.X., Wang. X.H. and Liu , Z., Biomed. Mater., 2010, 5: 054109
11 Blaker, J.J., Nazhat, S.N., Maquet, V. and Boccaccini, A.R., Acta Biomater., 2011, 7: 829
12 Mistry, A.S., Pham, Q.P., Schouten, C., Yeh, T., Christenson, E.M.and Mikos, A.G., J. Biomed. Mater. Res A, 2010, 92: 451
13 Armentano, I., Dottori, M., Fortunati, E., Mattioli, S. and Kenny, J.M., Polym. Degrad. Stab., 2010, 95: 2126
14 Guarino, V., Taddei, P., Di Foggia, M., Fagnano, C., Ciapetti, G. and Ambrosio, L., Tissue Eng. Part A., 2009, 15: 3655
15 Delabarde, C., Plummer, C.J.G., Bourban, P.E. and Manson, J.A.E. , Polym. Degrad. Stab., 2011, 96: 595
16 Hong, Z.K., Zhang, P.B., He, C.L., Qiu, X.Y., Liu, A.X. and Chen, L., Biomaterials, 2005, 26: 6296
17 Zhang, P.B., Hong, Z.K., Yu, T., Chen, X.S. and Jing, X.B., Biomaterials, 2009, 30: 58
18 Hong, Z.K., Qiu, X.Y., Sun, J.R., Deng, M.X., Chen, X.S. and Jing, X.B., Polymer, 2004, 45: 6699
19 Zhang, R.Y. and Ma, P.X., J. Biomed. Mater. Res., 1999, 44: 446

20 Xu, Y., Zhang, D., Wang, Z.L., Gao, Z.T., Zhang, P.B. and Chen, X.S., Chinese J. Polym. Sci., 2011, 29: 215
21 Pant, H.R., Neupane, M.P., Pant, B., Panthi, G., Oh, H.J. and Lee, M.H., Colloids. Surf. B. Biointerfaces, 2011, 88: 587
22 Mikos, A.G., Bao, Y., Cima, L.G., Ingber, D.E., Vacanti, J.P. and Langer, R., J. Biomed. Mater Res., 1993, 27: 183
23 Mikos, A.G., Thorsen, A.J., Czerwonka, L.A., Bao, Y., Langer, R. and Winslow, D.N., Polymer, 1994, 35: 1068
24 Chen, G.P., Ushida, T. and Tateishi, T., Mat. Sci. Eng C-Bio S., 2001, 17: 63
25 Zhang, P., Wu ,H., Lu, Z., Deng, C., Hong, Z. and Jing, X., Biomacromolecules, 2011, 12: 2667
26 Azevedo, H.S., Gama, F.M. and Reis, R.L., Biomacromolecules, 2003, 4: 1703
27 Dagang, G., Kewei, X. and Yong, H., J. Biomed. Mater. Res. A., 2008, 86: 947
28 Adachi, T., Osako, Y., Tanaka, M., Hojo, M. and Hollister, S.J., Biomaterials, 2006, 27: 3964
29 Ronca , A., Ambrosio, L. and Grijpma, D.W., Acta Biomater., 2013, 9: 5989
30 Lu, J.X., Flautre B., Anselme, K., Hardouin, P., Gallur, A. and Descamps, M., J. Mater. Sci. Mater. Med., 1999, 10: 111
31 Bai, F., Zhang, J., Wang, Z., Lu, J., Chang, J., Liu, J., Meng, G. and Dong, X., Biomed. Mater., 2011, 6: 015007
32 Boger, R.H., Palliat. Med., 2006, 20 Suppl 1: s17